High-Precision Model for Accurate Simulation of Trolleybus Grids: Case Study of Bologna

High-Precision Model for Accurate Simulation of Trolleybus Grids: Case Study of Bologna

Riccardo Barbone, Riccardo Mandrioli, Rudolf F. P. Paternost, Mattia Ricco, Gabriele Grandi
Department of Electrical, Electronic, and Information Engineering "Guglielmo Marconi" — DEI
Alma Mater Studiorum — University of Bologna, Bologna, Italy
{riccardo.barbone2, riccardo.mandrioli4, rudolf.paternost, mattia.ricco, gabriele.grandi}@unibo.it

***Abstract*—The integration of renewable sources to catenary-powered electric traction systems is a paramount step to satisfy sustainability and smart city objectives, albeit necessitating accurate simulations of the infrastructure. This paper presents an innovative trolleybus network simulator, characterised by the modularity of the catenary model and built on an intuitive graphical user interface that offers significant topological change flexibility. The model is distinguished by high precision and moderate processing effort, bridging the gaps of existing block-based simulation tools. A graphical analysis of the voltage distribution evaluated in a section of Bologna's trolleybus network shows the advances in precision of the proposed model.**

***Index Terms*—Catenary model, circuit modelling, electric mobility, smart DC grid, trolleybus, two-port network, urban transport**

I. Introduction

Trolleybus networks are re-emerging as a launchpad for carbon-neutral urban transport on the route to the development of smart cities. Public transit companies are being pressed to make the current infrastructure for electric traction sustainable and intelligent to meet the worldwide, environmentally friendly goals through 2050 [1]. The main components of a trolleybus system are two-wire overhead contact line (OCL) systems, also known as catenary, and DC traction power substations (TPSSs), such as uncontrolled rectifier substations (installed with a twelve-pulse rectifier). OCLs are divided into feeding sections (FSs) that can operate independently in the event of a fault to ensure the consistency of the traction system operation. Bilateral supply is provided for typical FSs [2]. In the case of two-way traffic, equipotential bonding (EB) systems, also known as voltage equalizers or current stabilizers, connects the two physically parallel OCLs at various adequately distributed points to create a double contact line (double-bifilar). By lowering the electrical resistance, especially farther from the TPSSs, the equipotentiality attained by these electrical connections tends to reduce catenary voltage drops.

To reduce greenhouse gas emissions, several actions may be addressed in the direction of smart and sustainable trolleybus systems. In addition to encouraging the use of public transport by optimising timetables in terms of regularity and frequency, the introduction of full-electric in-motion-charging trolleybuses is an important step towards low-carbon urban areas. Moreover, the DC catenary grid may work as a backbone for electric vehicles (EV) charging points, contributing to their deployment [3]–[6]. However, the aforesaid interventions may excessively burden the traction network, resulting in service interruptions in the worst-case scenario. Consequently, electrical support is required for the entire system. To avoid unwelcome OCL voltage decreases and to make the traction grid more environmentally friendly, stationary energy storage systems (SESSs) may be considered, as shown in [4], together with renewable energy sources. Therefore, it becomes increasingly important to carefully monitor the upgraded trolleybus network. The adoption of current infrastructure design methodologies becomes outdated, necessitating the formulation of advanced circuit modelling techniques.

A critical review of the literature on modelling techniques applicable to catenary DC traction systems is provided in [7]. From it it was found that nodal analysis-based methods, mainly developed via text-based coding, are capable of modelling catenary grids of complex topology, also providing elasticity in changing the number of in-transit vehicles [8], [9]. Briefly, all the infrastructure electrical elements are treated as grid nodes connected by branches, at which voltages and currents are respectively calculated with an iterative process. However, these approaches lack of a user-friendly man-machine interface, although they allow quite precise simulations without excessive time effort. In [10], a modular model was proposed in the Matlab-Simulink environment. Its modularity property still allowed for a simulation of multiple transit trolleybuses and a complex topology, overcoming the difficulties of existing graphical programming-based strategies in modelling the variability across time and space of the OCL electrical resistance as a result of vehicle motion [11]–[15]. The way the methodology adopted in [10] exploits the graphical interface attributes noteworthy flexibility to the respective circuit model. The only issue identified in the cited model concerns an inevitable spatial discretization in the vehicle position profiles, imposed by the way the model itself is built, whose refinement may lead to relevant computational effort (despite the abscence of root-finding iterative algorithms). Henceforth, this approach is referred to as the discrete method (DM). Given the importance of an intuitive man-machine interface especially for problems of this type, instead of resorting to nodal analysis-based models, this paper presents a method for augmenting the precision of modular multi-vehicle motion-based models while minimizing the time effort. Continuous method (CM) is the terminology adopted to denote such an approach. Bologna's trolleybus network was chosen as a case study, being arranged with FSs with simple and, mainly, complex topologies, with the latter emphasizing the potential of the devised simulation tool.

II. Exploring the Continuous Catenary Model

Similar to the model developed in [10], the goal of the model presented here is to replicate how trolleybus networks behave as a result of changes in vehicle positions over time, while also allowing for some flexibility in the selection of the number of transit vehicles. For this reason, a thorough examination of electrical substations is deemed unnecessary, and the Thevenin equivalent circuit is used to simplify the TPSS architecture [8]–[15]. Furthermore, the novel catenary model is decoupled from vehicle dynamics simulation. If the circuit element modelling the vehicle is just a time-dependent current generator, whose current profile is set as input to the model and can be obtained externally through an earlier simulation dedicated only to vehicle dynamics, the behavior of the catenary in terms of voltages and currents is not significantly affected. This trolleybus representation keeps the circuit linear, allowing for the development of the strategy suggested in this study.

Simulating the motion of the vehicle is the challenging aspect. As modelling the contact line resistance variability due to the trolleybus transit is not viable (see Section I) for accurate simulation goals, keeping the resistive grid configuration constant while logically allowing for the relocation of the vehicle electric absorptions is the basis of the new OCL model, as for the DM. However, the technique adopted for such a purpose is different for the CM and DM, as clarified in the following paragraphs.

A. From Step-Like to Ramp-Like Weight Function

In the DM, the main novelty consisted in building a modular catenary model by connecting in cascade a certain number ($N_{b,DM}$) of LEGO-like blocks (LBs), each of them representing a stretch of OCL, or span, with a fixed configuration [10]. The CM exploits such an approach, so that any OCL section of desired length and morphology could be modelled relatively easily and rapidly, and with remarkable flexibility. Fig. 1 shows the two circuit schematic drawings of the basic block implemented with the DM and the CM, respectively. For reasons better clarified later, the LB devised with the CM is referred to as tunable LB (TLB), practically speaking by virtue of the adjustable length of the modelled span. Basically, while the DM involves a number of LBs identical to each other (same half-span resistance R_{OCLhs} set for the entire model), with a current source (representing the vehicle) placed at the midpoint of the block itself, in the CM the value of the span resistances $R_{OCLs,k}$ ($k = 1,\ldots,N_{b,CM}$, where $N_{b,CM}$ is the number of blocks employed in the CM) for the positive and negative wires is determined TLB by TLB according to the length of the considered span. Furthermore, the TLB includes two current sources (absorbing currents $i_{gen\ l,k}$ and $i_{gen\ r,k}$) placed at the block ends.

The reason why the basic blocks in Fig. 1 have such a circuit topology can be understood by analysing Fig. 2. The discussion that follows is given by assuming that there is just one trolleybus T_j travelling along the analysed k-th OCL span with single-wire resistance $R_{OCLs,k}$. For easier visualization, the k-th span is made to be as long as the basic block utilized in the DM (see Fig. 1 (top)), yielding $R_{OCLs,k} = 2R_{OCLhs}$. Observe that just the positive wire's resistance is shown in Fig. 2. The circuit

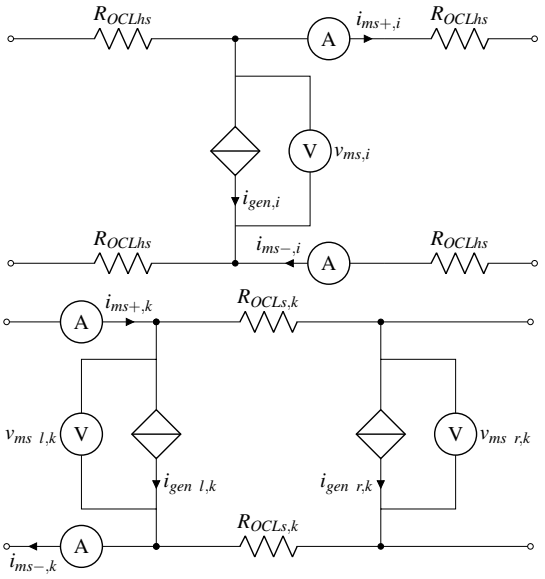

Fig. 1. Circuit schematic drawing of an LB (top) and of a TLB (bottom).

can be made simpler by virtually bringing the negative-wire resistance to the positive one (ignoring the negative wire) and doubling the positive-wire resistive contribution. This is because the resistances of the positive and negative poles are assumed to be equal and traversed by the same current. Due to the presence of the ground current, a non-uniform distribution of the equipotential bonding system, or any other electrical connection that produces asymmetry between the positive and negative poles, this hypothesis is invalid in practice. Later in this work, it will be shown that the same assumption can only be applied to structure the CM, while the real electric current mismatch between the positive and negative wires is regulated a posteriori.

To shift the time variability from the resistance of the contact line to the position of the absorption point of the electric vehicle, functions called weight functions are henceforth introduced, which distinguish the CM from the DM. The term "weight function" refers to the factor that multiplies the vehicle current by producing the contribution of the current generator(s) within the basic block (see Fig. 1).

Regarding the DM, the number of LBs is what forces the spatial discretization; it must be high enough for the corresponding contact line lengths to be sufficiently short so that their resistances can be deemed fixed. The actual location of the vehicle T_j inside the k-th span is rounded and referred to the position of the midpoint current generator within the LB representing that piece of catenary. In doing so, the equivalent line resistance observed by the active current source changes in a way that mimics the behavior of a real scenario. The weight function u defines whether the trolleybus is travelling within a certain LB, thus deciding on the activation of its midpoint current source. The DM relies on the following conditions:

$$\begin{cases} u_{i,j} = 0 & \text{if } T_j \notin LB_i \\ u_{i,j} = 1 & \text{if } T_j \in LB_i \end{cases} . \tag{1}$$

If T_j ($j = 1,\ldots,N_v$, where N_v is the number of transit vehicles) is within the i-th LB ($i = 1,\ldots,N_{b,DM}$), then the

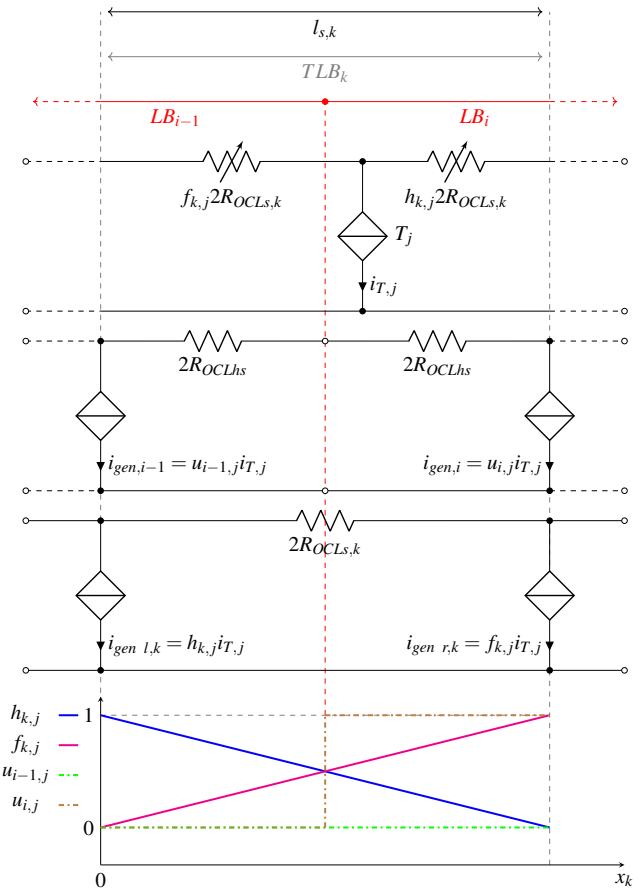

Fig. 2. Equivalent circuit configurations of the OCL span: real system (top), halves of adjacent basic blocks for the DM (middle), and basic block for the CM (bottom); weight functions behaviour (below the circuit schematic drawings).

weight function related to T_j, i.e., $u_{i,j}$, equals one, and the full current drawn by T_j ($i_{T,j}$) is assigned to $i_{gen,i}$; otherwise, $u_{i,j}$ equals zero. The lack of intermediate values of u in the interval [0,1] imposes a discretization dependent on the length of the resistive LB, so that the simulated trolleybus "jumps" from the midpoint of a block to that of the next one. The vehicle T_j in the example of Fig. 2 belongs to LB_i, therefore $u_{i-1,j}$ is set to zero and $u_{i,j}$ gains a unit value, in accordance with (1).

To increase the model precision, the CM can be developed by analysing in more detail the equivalent electric circuit representing the real system (top of Fig. 2). The in-motion vehicle can be viewed as a current generator acting as a slider between the positive and negative contact line wires. The equivalent resistance seen by the electrical node changes over time as it travels along with the displacement of the source. The moving current generator divides the positive wire resistance into two variable contributions so that the sum of the respective fractions of the overall span resistance always has a unit value. Equation (2) clearly shows that the fractions of OCL resistance are strongly related to the length of the relevant circuit branches:

$$\begin{cases} f_{k,j} = 1 - \frac{x_{k,j}}{l_{s,k}} \\ h_{k,j} = 1 - f_{k,j} = \frac{x_{k,j}}{l_{s,k}} \end{cases}, \tag{2}$$

where $x_{k,j}$ is the actual position of T_j with respect to the left end of the span under analysis (k-th), $l_{s,k}$ is the length of the span itself, which also corresponds to the distance between the neighbouring generators $i_{gen,i-1}$ and $i_{gen,i}$ (midpoint sources of LB_{i-1} and LB_i, respectively), $f_{k,j}$ and $h_{k,j}$ are complementary functions (their sum is equal to one) relative to the k-th span, regarded as further weight functions related to the portions of span resistance generated by T_j. The idea of the CM is to apply the same degree of variations ($f_{k,j}$ and $h_{k,j}$) of the two resistive contributions characterizing the k-th span to two current generators (left-end source $i_{gen\ l,k}$ and right-end source $i_{gen\ r,k}$, both part of the same TLB_k, i.e., bottom circuit diagram illustrated in Fig. 2) placed at its extrema, since dealing with electrical resistance variability is not practical for the above reasons.

Along the length of a TLB, the weight functions f and h behave linearly, ramp-like rather than step-like. The two-port network (2PN) theory is adopted to demonstrates the electrical equivalence of the TLB configuration proposed here and the system circuit layout (respectively, the bottom and top circuit schematic drawings of Fig. 2).

B. Tunable Lego-Like Basic Block

The basic block arrangement designed in the DM (see Fig. 1 (top)) is no longer viable for the CM due to the weight functions introduced in the CM itself. Indeed, adding electrical nodes between neighboring blocks would disrupt the continuity of the weight functions. Voltage equalizers or feeding points (feeders, reinforcing feeders (RFs), EV charging points, SESS connection points, and so on) would create electrical nodes, which compromise the distribution of current contributions between succeeding generators by causing the flow of additional currents. Due to this, the TLB embodies the circuit diagram in Figure 1 (bottom), with two current generators positioned laterally to represent all of the electrical absorption contributions of the vehicles crossing the span under analysis (appropriate logic was used to avoid the simultaneous activation of in-parallel generators at the boundary between adjacent basic blocks). By contrast, the DM did not find this issue, given that u has the form of an indicator function (see (1)) and that all the trolleybuses inside the OCL span were reported to the position of the midpoint current source via a rounding operation.

As previously hinted, fundamentals of circuit theory are resorted to in this work in order to demonstrate the correctness of the conversion of contact line resistance variability (real system) into current source variability (proposed model), i.e., to determine whether the weight functions reported in (2) are attributable to the two side current sources in the TLB. Basically, any stretch of catenary can be schematized as a 2PN, with into-port currents i_1 and i_2, and across-port voltages v_1 and v_2, as illustrated in Fig. 3. The left-end and right-end circuit diagrams in Fig. 3 are electrically equatable to one another if they have the same two-port equivalent Norton representation, depicted in the same figure. The key characteristics of the CM that make it effective at resolving the network are illustrated in the following paragraphs. For the analysis that follows, it is sufficient to focus on a single generic k-th basic block (TLB_k) due to the structure of the CM: hereinafter, the subscript k is omitted.

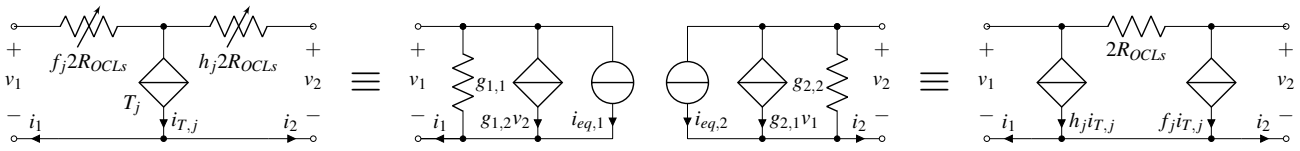

Fig. 3. Equivalence of the basic block for the CM (right) and the real system schematic drawing (left) with the two-port Norton equivalent circuit (middle).

1) Positive and negative wire imbalance management

Owing to the 2PN features, it is possible to evaluate the voltages and currents along a catenary stretch inside a TLB by assuming symmetry between the positive and negative wires. Hence, the resistance of the negative wire can be omitted, as illustrated in Fig. 2 and 3. However, the grounding system, along with any imbalanced electrical connection with the two wires, justifies the actual discrepancy between the respective currents.

Let us suppose that one has already determined the OCL currents at the desired m-th ($m = 1,\ldots,M$, where M is the number of measurement points) position within a given TLB under the hypothesis of wire symmetry. The following is an expression for the real currents $i_{OCL+,m}$ and $i_{OCL-,m}$ flowing along the positive and negative conductors, respectively:

$$\begin{cases} i_{OCL+,m} = i_{com,m} + i_{diff} \\ i_{OCL-,m} = i_{com,m} - i_{diff} \end{cases} , \tag{3}$$

where i_{diff} is the differential-mode current, which is the contribution to be accounted for matching the currents in the real system, and $i_{com,m}$ is the common-mode current, which is the current that has already been computed and is equal for both wires. Rearranging (3), one obtains

$$i_{diff} = \frac{i_{OCL+,m} - i_{OCL-,m}}{2} . \tag{4}$$

Referring to Fig. 1 (bottom), for any TLB the current values recorded by the ammeters are respectively allocated to $i_{OCL+,m}$ and $i_{OCL-,m}$. It is guaranteed that the difference between the values collected by the two ammeters is the same as between the two wires at any point within the TLB because in it there are no electrical connections other than the nodes due to the presence of vehicles across the positive and negative contact lines (the vehicles affect both pole currents equally). i_{diff} is deprived of the subscript m because of its independence from the measurement point location inside the considered TLB.

2) Analysis of voltages and currents along the OCL

Concerning the DM, the assessment of catenary voltages and currents was done at the LB level, which means that for each LB, only a pair of these two quantities were gathered using the associated voltmeter and ammeter, respectively (three quantities if considering the ammeter for measuring the negative-pole current, as shown in Fig. 1 (top)). To determine the distribution of the electrical parameters throughout the whole network, the readings are concatenated block by block.

The CM, instead, allows measurements to be performed at literally any number of points within each TLB, providing virtually limitless precision. As a result, since the electrical parameters are now set as input to the model, as will be explained further, the number of TLBs is no longer restricted by the quantity of electrical parameter acquisitions. This makes it possible to introduce fewer TLBs in areas of the grid without any topological element forming an electrical node, thus lowering the computational burden (for more details, refer to [16]). In essence, placing simply one TLB of the proper length is sufficient between any two neighboring electrical nodes; voltages and currents are then calculated inside it at any site selected in the input.

As a result of the linearity of the network, the superposition principle was applied to determine the OCL voltages and currents within each TLB by adding the outcomes derived by considering each trolleybus individually. Being the TLB a 2PN, the electrical parameters estimated in each block depend exclusively on the vehicles present in it, which is advantageous in terms of processing load (see [16]). The contribution of each vehicle external to the TLB is clustered in the across-port voltages of the TLB itself, measured by the left and right voltmeters illustrated in Fig. 1 (bottom). If there are no trolleybuses inside the TLB, then the common-mode current is only flowing because of the difference between $v_{ms\ l}$ and $v_{ms\ r}$. The term "circulating current" is used to describe the current:

$$i_c = \frac{v_{ms\ l} - v_{ms\ r}}{2R_{OCLs}} . \tag{5}$$

To determine the common-mode current and the voltage along the catenary, fundamental knowledge of circuit theory is needed, namely familiarity with Ohm's law and the current divider rule. Here, voltages and currents are calculated at the positions of the vehicles, which are gathered in the position vector fed as input to the model, as opposed to the DM where measurement points were established by the number of LBs. This is attributable to the dependence of the electrical parameters on the weight function f and h. The strategy is to increase the input vehicle position vector (and the associated input vehicle current vector I_T) with a view to adding more measurement sites, with a total of N_{vir} virtual trolleybuses absorbing zero current. Therefore, the total number of measurement points is $M = N_v + N_{vir}$ for N_v real vehicles.

$$I_{com} = [\mathrm{tri}_\mathrm{u}^\mathrm{s}(\mathbb{1}H^T) - \mathrm{tri}_\mathrm{l}(\mathbb{1}F^T)]I_T + i_c , \tag{6}$$

$$V_{OCL} = -2R_{OCLs}\{\mathrm{tri}_\mathrm{u}(FH^T) + [\mathrm{tri}_\mathrm{u}^\mathrm{s}(FH^T)]^T\}I_T + v_{ms\ l}H + v_{ms\ r}F \tag{7}$$

include matrix-based formulations employed by each TLB to calculate OCL common-mode currents (I_{com}) and voltages (V_{OCL}), respectively. tri_l and tri_u are functions that, once applied to the weight function matrices F and H, build the upper and lower triangular matrices, respectively, whereas $\mathrm{tri}_\mathrm{u}^\mathrm{s}$ creates a matrix that keeps the original matrix elements above the first superdiagonal; $\mathbb{1}$ is an all-ones column vector with M elements. The elements must be in a specific order for this matrix approach

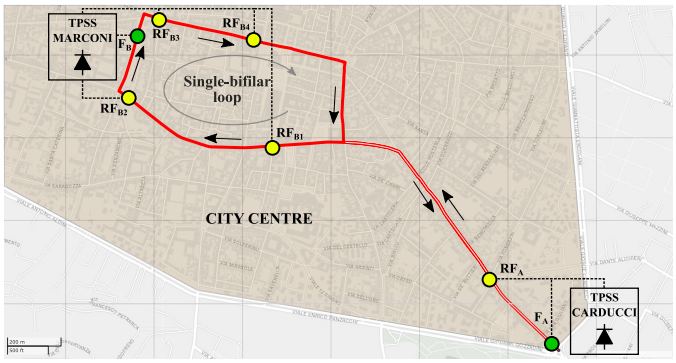

Fig. 4. Bologna's FS selected for the case study. The trolleybus routes (oriented by arrows) of the FS "Marconi-Carducci" are plotted together with TPSSs and supply points (connection points of line feeders with the OCL in green, i.e., F_A and F_B, and of RFs in yellow, i.e., RF_A, RF_{B1}, RF_{B2}, RF_{B3}, and RF_{B4}).

to work, which would obviously be hindered by the movement of the real vehicles in accordance with the input position profile. As a result, the CM demands matrix reordering every simulation step; further insights are provided in [16].

The non-null elements of F and H for each TLB are those that relate to the real or fictitious vehicles inside the TLB itself. As a result, there is no requirement for measurements concatenation like there was for the DM, but the contributions of all the TLBs in terms of OCL voltages and currents can be added together without overlapping each other. If $I_{com,k}$ and $V_{OCL,k}$ are the vectors containing the electrical parameters evaluated in the desired points along the entire catenary only with reference to the k-th TLB, the complete vectors I_{com} and V_{OCL} are obtained as follows:

$$\begin{cases} I_{com} = \sum_{k=1}^{N_{b,CM}} I_{com,k} \\ V_{OCL} = \sum_{k=1}^{N_{b,CM}} V_{OCL,k} \end{cases} . \tag{8}$$

Finally, the full distributions of the positive-wire and negative-wire OCL currents are obtained, respectively, by adding and subtracting the vector with the differential-mode currents (I_{diff}) found for all the TLBs from the I_{com} in (9):

$$\begin{cases} I_{OCL+} = I_{com} + I_{diff} \\ I_{OCL-} = I_{com} - I_{diff} \end{cases} . \tag{9}$$

III. Graphical Analysis and Discussion

In this section, the CM is first verified by comparison with the DM in terms of voltage and current distribution along one of the FSs that compose the trolleybus network in Bologna (the FS is considered in isolation for ease of analysis). The improvements in precision of the suggested model are further demonstrated by a graphical examination of the voltage distribution measured in a zoomed stretch of the same FS.

A. Verification of the Continuous Catenary Model

Fig. 4 depicts the geographical map of the bilaterally-fed FS "Marconi-Carducci" (FS MC). Due to the co-existence

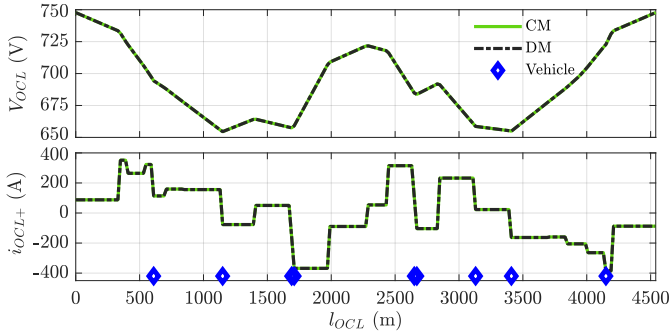

Fig. 5. OCL voltage (top) and current (bottom) distribution along FS MC.

of double-bifilar lines and single-bifilar loops, as well as the inclusion of several RFs dispersed along the catenary, FS MC owns a complex structure, increasing comparison effectiveness.

The simulation starting assumptions must be equivalent for the DM-CM comparison to sound right. First, in accordance with the decision to use a span length of 20 m inside each LB [10], the overall bifilar length was rounded to the nearest multiple of 20 m. As a result, the catenary length of FS MC, which is approximately 4541 m, was set to 4540 m (l_{OCL}). Any electrical component that was linked to the OCL was therefore positioned to the nearest multiple of 20 m. Secondly, the locations of the LBs' midpoint generators were taken by the virtual vehicles that represent the measurement sites in the CM. Furthermore, a moment in time was caught in which the actual running trolleybuses were also situated at the sites of the LBs' midway current sources in order to obtain the exact matching of the catenary voltages and currents using the two approaches.

The traction network data given in [10], where FS MC was extensively studied, were included in the simulation scenarios under consideration. In [17], FS MC was also investigated, and the idea of modernizing it with technology geared toward smart DC grids was accounted. In [18], other Bologna FS has been chosen as a case study for a system-level analysis.

Fig. 5 shows the voltage and current along the contact line of the FS MC, measured using both the DM and the CM at a moment in time when nine actual trolleybuses are positioned at specified locations determined by the aforementioned circumstances. It was decided to concentrate solely on the current flowing through the positive wire (i_{OCL+}) for the purposes of this study. Additionally, the open-circuit voltage at the TPSS terminals was set to 800 V (corresponding to the voltage on the AC side of the 12-pulse rectifier, i.e., 590 V). It is clear that the results of the DM and CM exactly match one another without any errors, as they should, despite the relevant presence of voltage angles and current steps due to the various electrical nodes spread all over the considered section. This proves the effectiveness of the CM and also confirms that catenary-powered electric traction grids can embrace the 2PN representation.

B. Precision Testing with Network Morphology Analysis

With a view to demonstrating the potential of the proposed circuit modelling technique in terms of precision, it was deemed helpful to investigate the complexity of the morphology of Bologna's trolleybus network. A similar analysis was done in

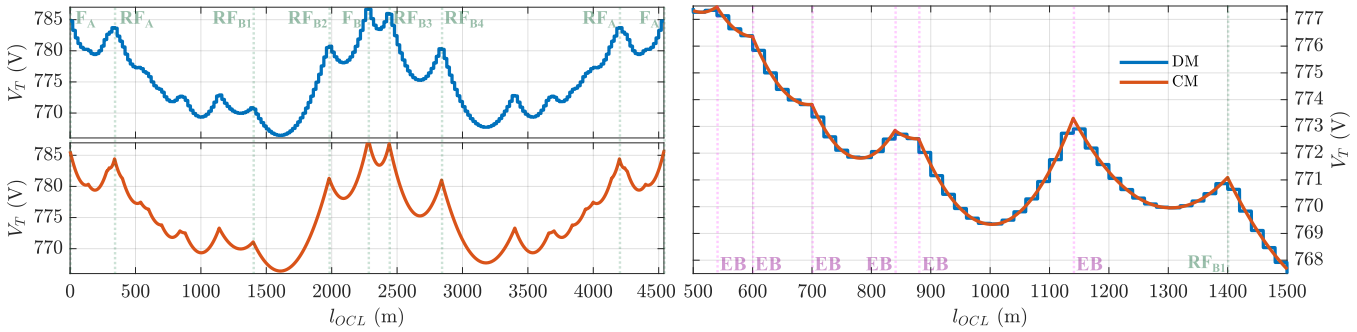

Fig. 6. OCL voltage distribution along FS MC obtained with the DM (top left) and CM (bottom left), and direct comparison between the two methods on a zoomed stretch of the same FS MC. The positions of feeders and RFs are shown in green or magenta according to the nomenclature adopted in Fig. 4.

[10] with the DM. For this purpose, the usefulness of assessing the voltage over time to which the vehicle is subjected as it travels along the FS MC was recognised. The graph in Fig. 6 displays the catenary voltage trend that one trolleybus (the only one in the FS MC for this study) sensed in its journey inside the FS as a function of its linearly time-varying position. If rounding the locations of any topological element (EB, feeder, and RF) to multiples of 20 m in the CM, it is more clear that the voltage determined through the CM itself follows the behaviour of the one of calculated with the DM (refer to the right graph in Fig. 6). The continuity of the OCL voltage profile achieved with the CM is emphasized with respect to the 20-m spatial discretization characterising the DM. Such a voltage trend continuity is especially evident in presence of single-bifilar sections without feeding points, i.e., at the larger voltage "valleys". The model-independent arbitrary precision that the CM can reach is also marked by the presence of sharp-edged peaks corresponding to the connection points of EBs (the slight increase in voltage in correspondence of such current stabilizers is attributable to the reduction in the catenary electrical resistance [10]), feeders, and RFs, in contrast with the step-like peaks obtained with the DM.

IV. Conclusion

A high-precision model of trolleybus networks was presented in this work. To prove its effectiveness, a direct comparison with a modular modelling technique published in the literature by the same authors was conducted. In contrast to the latter approach, the number of electrical parameter acquisitions is untied by the number of LEGO-like basic resistive blocks constituting the grid model, thus avoiding inevitable spatial discretization but also an excessive computational effort in case a more accurate simulation is demanded.

The two-port network concept demonstrates the reasonableness of the novel grid base element circuit, allowing for model-independent arbitrary precision in determining the network voltage and current distributions. Through a graphical analysis of a section of Bologna's trolleybus grid, while the line parameters match perfectly between the two compared methods if analogous conditions are applied, when simulating the morphology in detail the precise method exalts the continuity of the voltage profile as opposed to a stepped behaviour attributable to the discrete method.

References

[1] C. Fetting, "The european green deal," *ESDN Report, December*, 2020.

[2] A. A. Mohamed, A. A. Khan, A. T. Elsayed, and M. A. Elshaer, *Transportation Electrification: Breakthroughs in Electrified Vehicles, Aircraft, Rolling Stock, and Watercraft*. John Wiley & Sons, 2022.

[3] A. Shekhar, G. C. R. Mouli, S. Bandyopadhyay, and P. Bauer, "Electric vehicle charging with multi-port converter based integration in dc trolley-bus network," in *Proc. IEEE Int. Power Electron. Motion Control Conf.*, 2021, pp. 250–255.

[4] M. Weisbach, T. Schneider, D. Maune, H. Fechtner, U. Spaeth, R. Wegener, S. Soter, and B. Schmuelling, "Intelligent multi-vehicle dc/dc charging station powered by a trolley bus catenary grid," *Energies*, vol. 14, no. 24, 2021.

[5] M. Bartłomiejczyk, L. Jarzebowicz, and R. Hrbáč, "Application of traction supply system for charging electric cars," *Energies*, vol. 15, no. 4, 2022.

[6] I. Diab, G. R. C. Mouli, and P. Bauer, "Increasing the integration potential of ev chargers in dc trolleygrids: A bilateral substation-voltage tuning approach," in *Proc. Int. Symp. Power Electron. Elect. Drives Automat. Motion*, 2022, pp. 264–269.

[7] R. Barbone, R. Mandrioli, M. Ricco, R. F. P. Paternost, V. Cirimele, and G. Grandi, "Modelling trolleybus networks: a critical review," in *Proc. Int. Symp. Power Electron. Elect. Drives Automat. Motion*, 2022, pp. 258–263.

[8] A. Capasso, M. Ceraolo, R. Lamedica, G. Lutzemberger, and A. Ruvio, "Modelling and simulation of tramway transportation systems," *J. Adv. Transp.*, vol. 2019, pp. 1–8, 2019.

[9] I. Diab, A. Saffirio, G. R. C. Mouli, A. S. Tomar, and P. Bauer, "A complete dc trolleybus grid model with bilateral connections, feeder cables, and bus auxiliaries," *IEEE Trans. Intell. Transp. Syst.*, vol. 23, no. 10, pp. 19 030–19 041, 2022.

[10] R. Barbone, R. Mandrioli, M. Ricco, R. F. Paternost, V. Cirimele, and G. Grandi, "Novel multi-vehicle motion-based model of trolleybus grids towards smarter urban mobility," *Electronics*, vol. 11, no. 6, 2022.

[11] H. Alnuman, D. Gladwin, and M. Foster, "Electrical modelling of a dc railway system with multiple trains," *Energies*, vol. 11, no. 11, 2018.

[12] F. Mao, Z. Mao, and K. Yu, "The modeling and simulation of dc traction power supply network for urban rail transit based on simulink," *J. Phys. Conf. Ser.*, vol. 1087, no. 4, p. 042058, sep 2018.

[13] F. Fan and B. G. Stewart, "Power flow simulation of dc railway power supply systems with regenerative braking," in *Proc. IEEE Mediterr. Electrotech. Conf.*, 2020, pp. 87–92.

[14] G. Stana and V. Brazis, "Trolleybus motion simulation by dealing with overhead dc network energy transmission losses," in *Proc. Int. Sci. Conf. Electr. Power Eng.*, 2017, pp. 1–6.

[15] A. Jakubowski, L. Jarzebowicz, M. Bartłomiejczyk, J. Skibicki, S. Judek, A. Wilk, and M. Płonka, "Modeling of electrified transportation systems featuring multiple vehicles and complex power supply layout," *Energies*, vol. 14, no. 24, 2021.

[16] R. Barbone, R. Mandrioli, M. Ricco, and G. Grandi, "Development of a high-precision and flexible model for accurate simulation of trolleybus grids," *IEEE Access*, Early Access, doi: 10.1109/ACCESS.2023.3265379.

[17] R. Barbone, R. Mandrioli, M. Ricco, R. F. P. Paternost, F. L. Franco, and G. Grandi, "Flexible and modular model for smart trolleybus grids," in *Proc. IEEE Int. Conf. Compat., Power Electron. Power Eng*, 2022, pp. 1–6.

[18] R. F. Paternost, R. Mandrioli, R. Barbone, M. Ricco, V. Cirimele, and G. Grandi, "Catenary-powered electric traction network modeling: A data-driven analysis for trolleybus system simulation," *World Electr. Veh. J.*, vol. 13, no. 9, 2022.